A Real-Time Ultrasound Time-Domain Correlation Blood Flowmeter: Part I—Theory and Design

I. A. Hein, *Member, IEEE,* J. T. Chen, *Member, IEEE,* W. K. Jenkins, *Fellow, IEEE,* and W. D. O'Brien, Jr., *Fellow, IEEE*

***Abstract*— A real-time ultrasound time-domain correlation (UTDC) blood flowmeter has been developed. Real-time performance has been achieved through the implementation of a custom-designed high-speed residue-number system (RNS) hardware correlator. The flowmeter is interfaced to a commercial ultrasound imager and can produce one-dimensional velocity versus range graphs at a rate of three per second. It has been validated in a blood flow phantom under a variety of conditions along with *in vivo* measurements in the human carotid artery. Part I of this work describes the theory of the time-domain correlation technique, design and implementation of flowmeter hardware, and the important correlation parameters which affect the performance of the flowmeter. Part II presents selection of the optimal real-time correlation parameters and experimental results obtained using the system and parameters.**

NOMENCLATURE

c	Speed of sound.
Δ	Echo signal spacing used in individual flow velocity calculations.
$\Delta_{\max}$	Maximum echo signal spacing used in flow velocity calculation. Δ ranges from one to $\Delta_{\max}$.
E	Number of ultrasound echo signals used in producing a flow velocity estimate.
EL	Echo length in digitized points.
EP	Number of echo signal pairs used in producing a flow velocity estimate. Determined by E an $\Delta_{\max}$.
M	Product of all individual residue number system moduli.
m_{p_i}	$= M/p_i$.
p_i	Residue number system moduli.
$R()$	Correlation function.
R_i	Range increment. Determines the axial measurement spacing of flow velocity profiles.
$R_{\max}$	Value of the correlation function at the peak.
$S_{\max}$	Local shift value of maximum correlation coefficient $R_{\max}$.
$SR_{\min}, SR_{\max}$	Search range limits used in the maximum correlation search routine.
S_p	Preshift estimate for Δ's > 1.
T	Pulse repetition period.
τ	Time shift.
θ	Angle between ultrasound beam axis and vessel axis.
$V_{a\Delta}$	Individual axial flow velocity calculated with a given Δ.
V_a	Averaged axial flow velocity estimate produced from $\Delta_{\max}$ Δ individual flow velocity estimates.
V_T	Angle-corrected true flow velocity estimate.
x_{p_i}	Residues of a data word for modulus p_i.

Manuscript received January 24, 1992; revised May 11, 1993; accepted May 13, 1993. This work was supported by the National Institutes of Health, and the National Heart, Lung, and Blood Institute under Grant HL39704.

I. A. Hein was with the Bioacoustics Research Laboratory, Department of Electrical and Computer Engineering, University of Illinois, Urbana, IL. He is now with Bio-Imaging Research, Inc., Lincolnshire, IL 60069.

J. T. Chen was with the Coordinated Science Laboratory, Department of Electrical and Computer Engineering, University of Illinois, Urbana, IL. He is now with the Los Alamos National Laboratory, MS J-580, Los Alamos, NM 87545.

W. K. Jenkins is with the Coordinated Science Laboratory, Department of Electrical and Computer Engineering, University of Illinois, Urbana, IL 61801.

W. D. O'Brien, Jr. is with the Bioacoustics Research Laboratory, Department of Electrical and Computer Engineering, University of Illinois, Urbana IL 61801.

IEEE Log Number 9211584.

I. INTRODUCTION

THE KNOWLEDGE of the volumetric blood flow rate is an important quantity in the diagnosis of various diseases and trauma as well as in cardiovascular research. Volume blood flow is one of the best indicators of available oxygen and also of the ability of the heart to maintain normal body processes. Classical methods of blood flow measurement, such as Fick's method, dye dilution, and angiographic techniques, are invasive and can be potentially harmful to the patient, particularly if the patient is already very ill. Non-invasive blood flow measurement techniques are thus highly desirable.

The use of ultrasound to noninvasively measure blood flow has become a standard clinical practice. The most popular ultrasonic measurement method is the well-known Doppler technique. The Doppler technique estimates blood flow velocity from the echo signals by analyzing their frequency change. Mathematically, the Doppler equation is expressed as

$$V_D = \frac{f_d c}{2 f_t \cos(\theta)} \tag{1}$$

where V_D is the velocity, f_t is the frequency of the transmitted signal, f_d is the Doppler shift (received frequency minus the

transmitted frequency), c is the speed of sound in the medium, and θ is the angle between the sound beam and the axis of blood flow [1].

The major drawback of Doppler techniques is that the Doppler shift f_d is never a single frequency but a band of frequencies with a spectrum similar to that for band-limited random noise [2]. Problems arise with Doppler measurements because there are factors which can affect the shape of the Doppler frequency band that are not related to blood flow, such as frequency-dependent scattering and attenuation in tissue [3], [4]. For these reasons, Doppler ultrasound tends to be more of a qualitative than quantitative blood flow measurement method.

Recently, there has been a growing interest in using time-domain instead of frequency-domain methods to extract motion information from reflected ultrasound echoes. Time-domain correlation techniques have theoretical advantages over Doppler techniques, which makes them potentially more accurate and precise. A detailed comparison of time-domain and Doppler, and the potential advantages of using time-domain instead of Doppler, has been presented in [5]. Ultrasound time-domain correlation (UTDC) techniques have been developed to assess tissue motion [6]–[11] as well as for blood flow [12]–[22]. Previous research by us has shown that UTDC techniques can be used to measure constant and pulsatile flow in a flow phantom with an accuracy of better than 20% [6], [15].

One problem with time-domain methods is that they tend to be computationally very intensive, and measurements have generally been restricted to off-line analysis. In order to be clinically useful, an ultrasonic blood flowmeter should be capable of producing results in real-time. Recently, a real-time UTDC blood flowmeter has been constructed [23], [24]. It incorporates a high-speed residue-number system correlator, which replaces hardware multipliers with high-speed lookup tables stored in ROM. The correlation parameters used in making velocity estimates have been selected for speed and accuracy. The result is a UTDC flowmeter capable of producing a flow velocity versus range profile in real time (every 0.34 s). Previous UTDC blood flowmeters [15], [23] required up to 90 s in order to compute the same result. This paper presents the theory and design of the real-time UTDC flowmeter. The real-time flowmeter has been extensively validated in a blood flow phantom under various conditions, such as the presence of scattering media and multiple vessels, and has the same accuracy and precision as the previous systems. The performance of the flowmeter is presented in Part II of this work [24].

II. Ultrasound Time Domain Correlation Technique

A. Time-Domain Velocity Measurement Concept

The ultrasound time-domain flowmeter concept is illustrated in Fig. 1. Here an ultrasound transducer is oriented at some measurement angle θ with respect to a blood vessel. At time $t = t_0$, a blood cell scatterer is located in position 1. If an ultrasonic pulse is transmitted at time $t = t_0$, then it will take a round trip time t_1 to leave the transducer, get reflected, and return to the transducer. If another ultrasonic pulse is initiated T seconds later at time $t = t_0 + T$, then the scatterer will have moved to position 2 and the round trip transit time will be t_2. The axial distance d_a the scatterer has moved in the direction of the ultrasound beam can be calculated from the difference in transit times of the two ultrasound pulses:

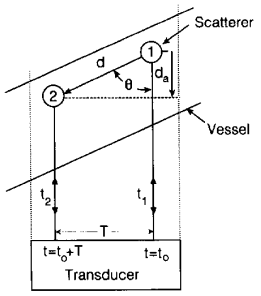

Fig. 1. Ultrasound time-domain flowmeter concept. The velocity of a scatterer can be calculated from the transit times of two ultrasonic pulses reflected from the scatterer at two positions along the vessel.

$$d_a = (t_1 - t_2)c/2 \tag{2}$$

where c is the speed of sound in the medium. The distance d the scatterer has moved within the vessel is $d_a/\cos(\theta)$, where θ is the transducer measurement angle (also called the Doppler angle). Since velocity is distance/time, the true angle-corrected scatterer velocity is (assuming $V_T \cos(\theta) \ll c$)

$$V_T = \frac{(t_1 - t_2)c}{2T\cos(\theta)} \tag{3}$$

This time-domain equation is very similar to the Doppler equation (1) except that it has a change in time in the numerator instead of a change in frequency, and the pulse repetition period in the denominator instead of the transmitted frequency. The change in time $t_1 - t_2$ is referred to as the time shift and is denoted by the variable τ.

In the real-life situation, the actual ultrasonic echo is due to all of the scatterers within the ultrasound beam, as illustrated in Fig. 2. In this figure E_1 is the echo signal which includes part of the signal that is due to volume 1 (V_1), which has almost moved out of the ultrasound beam due to motion of the scatterers. E_2 is the echo signal which includes part of the signal that is due to volume 2 (V_2), which is shown totally within the ultrasound beam. If the pulse repetition period is chosen such that some of the original scatterers remain common to both pulses (shaded areas of V_1 and V_2), then these volume sections will produce similar sections of echo signals in E_1 and E_2. These similar sections of echo signals will be displaced in time from each other by the time shift τ. The shape of the ultrasound signal reflected from a small volume of flowing blood is determined by such factors as the local density and orientation of blood cell scatterers within the volume, which fluctuate randomly around a mean value. This implies that any two different volumes of blood will produce a different reflected ultrasound echo shape due to the instantaneous random nature of the scatterers (ultrasound

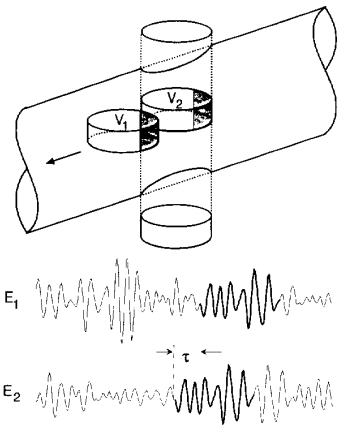

Fig. 2. The actual ultrasound echo signal is due to all scatterers within the ultrasonic beam. E_1 is the echo signal which includes part of the signal that is due to volume 1, which has almost movedout of the beam. E_2 is the echo signal which includes part of thesignal due to volume 2, still within the beam. The common sections of V_1 and V_2 (shaded) will produce similar sections of echo signal in E_1 and E_2.

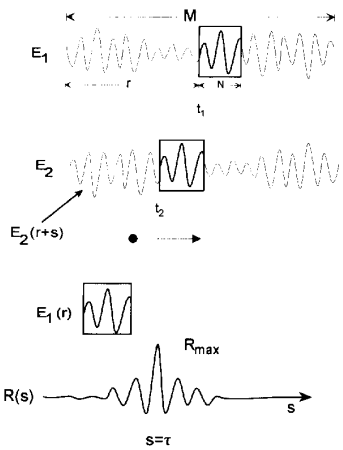

Fig. 3. The digital correlation procedure consists of removing a window of width N at desired range r from one echo signal E_1 and correlating it at different locations s along another echo signal E_2. The value of s producing the maximum $R(s) = R_{\max}$ corresponds to $s = \gamma$.

reflected from blood is statistically a Gaussian random variable [25]). Thus, any small volume of blood cell scatterers will have its own unique ultrasonic footprint, and the common sections of echo signals in E_1 and E_2 will represent reflections from the same group of blood cell scatterers. If τ can be determined, then (3) can be used to calculate the velocity of a particular blood scatterer group.

The time shift τ is estimated by correlating different echo signals with each other. If $E_1(t)$ and $E_2(t)$ represent signals received at different times from a moving scatterer, then the correlation can be pictured as shifting E_1 back in time by some value of s and multiplying by E_2 to produce the correlation coefficient $R(s)$. Mathematically this can be expressed as

$$R(s) = \int_t E_1[t+s]E_2[t] \tag{4}$$

The value of s which produces a maximum in the correlation function $R(s)$ corresponds to the time shift $s = \tau = t_1 - t_2$ and (3) can be used to calculate the scatterer velocity.

Digital Correlation If the ultrasound echo signals are digitized and stored, the time shift τ can be estimated at different ranges by a process of digitally shifting and correlating to find the value of s producing the maximum $R(s) = R_{\max}$. The digital correlation process for digitized echo signals is shown in Fig. 3. The RF echo signals E_1 and E_2 are digitized for a length of M points. A digital length is related to a distance in tissue by $d_t = pT_s c/2$, where d_t is the equivalent distance in tissue, p is the digital length in number of sample points, T_s is the A/D sampling period, and c is the speed of sound. A window of length N samples is windowed out from E_1 at a distance r points (corresponding to the desired range) from the beginning of the echo signal. The window length N, along with the transducer beam width, define the sample volume size (V_1 and V_2 in Fig. 2) and thus the axial resolution of flow velocity estimation. This window is correlated with equivalent length windows at different locations $r+s$ ($-r \le s \le M - N$) along E_2 where s is the shift location in E_2 with respect to r of E_1. The value of s at the peak of the correlation function $R(s)$ corresponds to the time shift τ in units of the A/D sampling period, and the value of the $R(s)$ at the peak is referred to as $R_{\max}$. The normalized correlation coefficient $R(s)$ is given by the equation

$$R(s) = \frac{\sum_{i=0}^{N-1} E_1[r+i]E_2[r+s+i]}{\sqrt{\sum_{j=0}^{N-1}(E_1[r+j])^2 \sum_{k=0}^{N-1}(E_2[r+s+k])^2}} \tag{5}$$

where E_1 and E_2 are the base addresses of the digitized echo signals. This equation estimates the similarity of the data within the two windows and produces a value between $+1.0$ and -1.0. A value of $+1.0$ corresponds to identical windows, zero indicates the echoes are maximally dissimilar, and -1.0 indicates the windows are exact reflections of each other about the amplitude axis. The correlation search procedure searches for the maximum positive value of the correlation function, thus $R_{\max}$ generally varies between zero and one.

B. Weighted Axial Velocity Measurement

It has been shown that the precision (defined as the standard deviation divided by the mean) of the UTDC technique is dependent on the time shift τ [13], which is directly determined by the PRF. For a given velocity, a faster PRF will produce a smaller time shift, since the scatterers will have less time to move between pulses. Since the blood scatterer velocity may change, such as with pulsatile flow in the human body, a single PRF may have optimal precision at one scatterer velocity but poor precision at a faster or slower velocity. A method of effectively varying the PRF without physically doing so is to exploit the fact that the scatterers remain within the ultrasound beam for more than just two pulses [14]. If the scatterer remains within the beam for P ultrasonic pulses, then any two echo signal pairs can be used as an independent velocity measurement. If Δ is defined as the echo signal pair spacing, then $\Delta = 1$ corresponds to correlations between adjacent echo signals; a $\Delta = 2$ corresponds to every other echo signal, etc.;

up to a maximum echo signal spacing $\Delta_{\max} = P - 1$. Thus for any two echoes i and j ($j > i$), $\Delta = j - i$ and the time shift $\tau_\Delta = t_j - t_i$. The axial velocity $V_{a\Delta}$ can be calculated for a given echo signal spacing from

$$V_{a\Delta} = \frac{c\tau_\Delta}{2\Delta T} \tag{6}$$

where c is the speed of sound and T is the pulse repetition period. For P echoes, there will be $P-\Delta$ velocity estimates for each Δ. These can be averaged to produce a single velocity estimate $\overline{V}_{a\Delta}$ for each Δ.

In general, for a given velocity, a smaller Δ will produce a smaller time shift, since the scatterers will have less time to move between pulses. Since the blood scatterer velocity may change, such as with pulsatile flow, a given Δ may have optimal precision at one scatterer velocity but poor precision at a faster or slower velocity. To produce an optimal velocity estimate from the Δ number of $\overline{V}_{a\Delta}$a values, a weighted average is performed:

$$V_a = \sum_{\Delta=1}^{\Delta_{\max}} W_\Delta \overline{V}_{a\Delta} \tag{7}$$

where V_a is the final axial velocity estimate for a range and W_Δ is a weighting factor determined by the variance of the individual $\overline{V}_{a\Delta}$ estimates. Those estimates with low values of variance are weighted more heavily than those with a higher variance, thereby producing a more precise estimate than if the $\overline{V}_{a\Delta}$ would simply have been averaged [14]. The true angle-corrected velocity estimate is then $V_T = V_a/\cos(\theta)$, where θ is estimated from the ultrasound image [24].

Once the optimal velocity has been estimated at the desired ranges, a one-dimensional flow velocity versus range profile can be generated.

III. UTDC Real-Time System Hardware

Fig. 4 shows the setup of the real-time UTDC system, which consists of an ATL MK500 imager with a 5-MHz transducer, a 33-MHz 486 PC, and a custom-built ultrasound data acquisition and residue number correlator (UDA-RNC) system. The UDA-RNC system consists of two main subsystems: a TRW 50-MHz A/D and bus expander [23] interfaced to a hardware RNS correlator [26], [27]. The RF and position signals are tapped from the MK500 and the RF signals are digitized and placed into the RNS correlator memory. The correlator produces time shift values, which are sent to the 486 PC. The 486 PC performs flow velocity calculations from the time shifts and produces the flow velocity versus range profiles.

A. A/D Subsystem

The A/D subsystem is based on the bus-expander design [6]. It is capable of digitizing and consecutively storing programmable-length echo signals in 256K of 25-ns dual port memory. The TRW A/D digitizes at 50 MHz, has an input range of +0.5–−0.5 V, and an 8-bit output. The 8-bit output from the A/D is expanded into 32 bits by the bus expander. The bus expander design was necessary because fast enough memory was not available to directly store data from

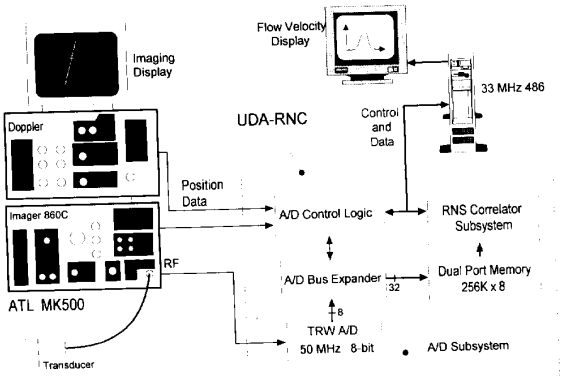

Fig. 4. Block diagram of the real-time UTDC blood flowmeter. RF ultrasound signals from the commercial imager are digitized at 50 MHz and a high-speed RNS correlator is used in conjunction with a 486 PC to perform correlation analyses on the echo signals. The final result is a plot of the flow velocity versus range at the desired location on the ultrasound image.

the 50-MHz A/D. The bus expander writes four consecutive 8-bit bytes into the dual-port memory every 80 ns. The dual-port memory has two separate address and data busses and two copies of the ultrasound data are stored at acquisition time. This allows the RNS correlator to access two echo signals simultaneously for correlation instead of requiring two separate steps.

B. Residue Number System (RNS) Correlator

Previous research [13] has shown that for 5-MHz RF ultrasound digitized at 50 MHz, a 40-point correlation window (corresponding to an axial window of 0.6 mm) is an optimal compromise between range resolution and measurement precision, where the range resolution is the correlation window convolved with the transmitted pulse length. The RNS correlator performs the following basic 40-point digital correlation on two echo windows:

$$R(a,b) = \sum_{i=0}^{39} E_1[a+i] * E_2[b+i] \tag{8}$$

where E_1 and E_2 are the base addresses of the echo signals, a is the location of the correlation window within the first echo signal, and b is the location of the correlation window within the second echo signal.

Residue Number System implementation RNS arithmetic is extremely efficient in performing high-speed addition and multiplication and is ideally suited for the UTDC digital correlation function [28]. The concept behind using RNS arithmetic is to replace hardware multiplications by addition and high-speed lookup tables stored in ROM. Typically, addition and access of lookup tables can be performed faster than multiplying. RNS accomplishes this by breaking down data words of a given length to a number of smaller length words called residues. The number and size of the residues are dependent on the desired dynamic range of the system. These residues are integers of different moduli and must be pairwise prime. A data word is encoded into residues of these moduli

by the equation

$$x_{p_i} = \begin{cases} |X|_{\text{mod}p_i} & x \geq 0 \\ p_i - |X|_{\text{mod}p_i} & x < 0 \end{cases} 1 \leq i \leq L \qquad (9)$$

where X is the original length data word, p_i's are the moduli, x_{p_i}'s are the residues of the moduli, and L is the total number of moduli. Residues can be reconstructed back into a natural number using the Chinese Remainder Theorem [28]:

$$Y = \left| \sum_{i=1}^{L} m_{p_i} |m_{p_i}^{-1} y_{p_i}|_{\text{mod } p_i} \right|_{\text{mod M}} \qquad (10)$$

where Y is the natural number base 10, $M = p_1 p_2 \cdots p_L, m_{p_i} = M/p_i$, and $m_{p_i}^{-1}$ is the inverse of m_{p_i} such that $|m_{p_i} m_{p_i}^{-1}|_{\text{mod } p_i} = 1$. An RNS correlation example is given in the Appendix.

Dynamic Range: For this application, the data word length is 8 bits and the correlation window is 40 samples wide. A theoretical dynamic range of 21 bits (8-bit signed value * 8-bit signed value * 40) is required. This can be covered by four 6-bit moduli: $p_1 = 59$, $p_2 = 61$, $p_3 = 63$, and $p_4 = 64$ (64 is allowed since the largest residue from a mod 64 number is 63). This implementation has a 24-bit dynamic range and commonly-available high-speed 8192 x 8 ROM's can be used for the lookup tables.

The theoretical maximum dynamic range (21 bits) is required if the situation occurs where both echo signal windows consist of only one value, that where the A/D is clipped at either +0.5 or −0.5 V. In reality, reflected ultrasound signals from blood have a zero-mean Gaussian distribution [25], and the gain of the RF input is adjusted such that it is within the dynamic range of the A/D (no clipping). This means the theoretical maximum dynamic range of 21 bits will never be approached. The minimum required realistic dynamic range was estimated theoretically by correlating identical echo windows with a Gaussian distribution, where the standard deviation was the largest possible which would not produce clipping of the A/D. It was found that 16 bits can adequately cover this range. This is significant because 16 bits is the width of the PC's data bus, and a single read function (instead of two) can be used to receive a value from the correlator. Sixteen bits can be theoretically covered by three 6-bit moduli instead of four. However, in order to have the maximum amount of flexibility for future expansion, the system was designed to accommodate the entire 21-bit dynamic range, which is scaled down to 16 bits in the RNS decoder.

The overall correlator architecture is shown in Fig. 5. The correlator consists four RNS correlator channels (one for each modulus). Each channel consists of a pipelined architecture which performs an add and a multiply simultaneously for 40 samples. The arithmetic operations in the correlator channels are performed using ROM lookup tables. The individual RNS arithmetic is performed simultaneously within the four channels. The results from the four correlator channels are reconstructed into a 16-bit binary value by the RNS decoder and sent to the 486 PC for processing.

Fig. 6 shows a block diagram of a single RNS correlator channel. The residue-encoding ROM's are 512 x 8 with a response time of 25 ns and the add and multiply ROM's are 4096 x 6-bit with a 40 ns response time. Two 8-bit data values from the dual-port memory (E_1 and E_2) are encoded into two 6-bit modp_i values. The values are multiplied using lookup tables, producing a 6-bit modp_i result. This result is RNS added with the previous sum and saved in the sum register. The final RNS result y_{p_i} for this channel is completed after 40 data points have been processed.

A block diagram of the residue to binary decoder is shown in Fig. 7. The decoder produces a result scaled from 24 to 16 bits. This is done with the least amount of scaling error by first scaling by a modulus to 18 bits and discarding the two least significant bits. The y_{p_i}'s are decoded and scaled into a single 18-bit value by precalculating two subtotals stored in ROM lookup tables. The scaled output, denoted Y_s is produced by implementing the Chinese Remainder Theorem as follows

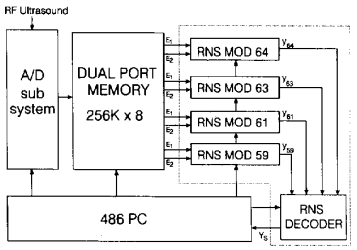

Fig. 5. Block diagram of the RNS correlator subsystem. Each RNS channel simultaneously accesses two echo signals and performs RNS correlations. The outputs of the channels are combined into a 16-bit result by the RNS decoder.

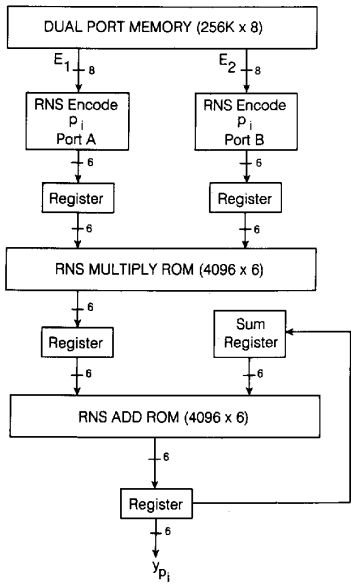

Fig. 6. Block diagram of a single mod π RNS correlator channel. Two 8-bit echo signal values are encoded into 6-bit moduli and a 4096 x 6 lookup-table ROM is used for multiplies. The multiplied values are summed over 40 points to produce the mod p_i value for this channel.

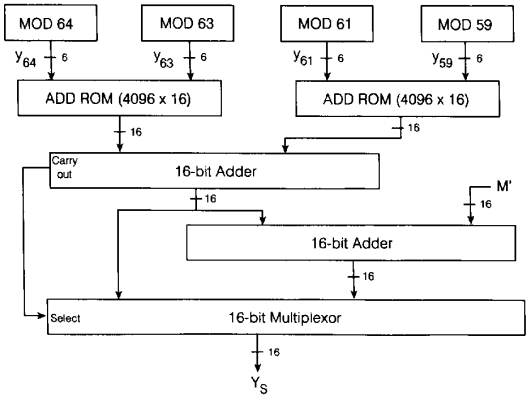

Fig. 7. Block diagram of the residue-to-binary decoder. An 18-bit scaled Chinese Remainder Theorem is implemented by precalculating two subtotals stored in ROM. The two least significant bits are discarded to produce a 16-bit result.

$$Y_s(y_{64}, y_{63}, y_{61}, y_{59}) = \begin{bmatrix} (y_{64}\hat{m}_{64}^{-1}\hat{m}_{64s} & + & y_{63}\hat{m}_{63}^{-1}\hat{m}_{63s}) \\ & + & \\ (y_{61}\hat{m}_{61}^{-1}\hat{m}_{61s} & + & y_{59}\hat{m}_{59}^{-1}\hat{m}_{59s}) \end{bmatrix}_{\text{mod } \hat{m}_{63}} \quad (11)$$

$\hat{m}_i = M/m_{p_i} (M = m_{64}m_{63}m_{61}m_{59})$
$\hat{m}_{p_i}^{-1}$ is the multiplicative inverse of $\hat{m}_{p_i}$ modulo m_{p_i}
$\hat{m}_{64s} = \hat{m}_{64}/m_{63}, \hat{m}_{63s} = \hat{m}_{63}/m_{63}, \hat{m}_{61s} = \hat{m}_{61}/m_{63}$, and $\hat{m}_{59s} = \hat{m}_{59}/m_{63}$

where the terms in the parentheses are precalculated and stored in the two 4096 x 16 ROM's and $\hat{m}_{63}$ denotes the 18-bit scaled dynamic range. The two scaled subtotals are then added together and checked for overflow. If an overflow occurs, the result is taken modulo m_{63}. To save time, both the result and the result modulo m_{63} are calculated and the correct one selected based on the carry out of the 16-bit adder. The final output of the correlator is a 16-bit value corresponding to $R(a, b)$ in (8).

The speed of a 40-point correlation is determined by the speed of the memory and ROM's and the pipeline architecure. The pipeline architecure allows a 40 point correlation to be processed in 48 50-ns clock pulses, for a total processing time of 2.4 μs. As a comparison, the hardware correlator used in previous systems was based on a commercially-available TRW hardware multiplier, and was capable of multiplying two samples and adding the result to an accumulator every μs. Thus a 40-point correlation required approximately 40 μs, as compared to 2.4 μs for the current RNS correlator.

C. Maximum Correlation Search

The process of finding the shift value where the maximum correlation occurs consists of sending a shift s to the correlator, calculating the correlation coefficient according to (5) and repeating the process until the maximum correlation coefficient is found. Three calls to the RNS correlator are made for each normalized correlation: $R(a, b)$, $R(a, a)$, and $R(b, b)$ where $a = E_1[r]$ and $b = E_2[r+s]$ (one for the numerator and two for the squared quantities in the denominator of (8)). In order to save processing time for Δ's larger than one, an initial preshift S_p is estimated from the value of τ found from the previous Δ estimate. The shifting-correlating process is then performed at N points about S_p, beginning at $S_p + SR_{\min}$ and ending at $S_p + SR_{\max}$, where $SR_{\min}$ and $SR_{\max}$ define the search range limits and $N = SR_{\max} - SR_{\min}$. The location of the maximum correlation coefficient will be found at a local shift $s_{\max}$, and the total time shift $\tau = S_p + s_{\max}$. The true value of τ will in general not be restricted to integral increments of the sampling period, hence a parabola is fit to the maximum shift and its two neighboring points to estimate the fractional part of τ. This is the same method used by Embree and O'Brien [14].

D. Correlation Parameters

The real-time system has been designed to allow as many of the correlation parameters to be varied as possible. The A/D subsystem can be programmed with the number of acquired echo signals and the acquired echo signal length. $\Delta_{\max}$, the processed number of echoes E, the processed echo length EL, the range increment R_i, and the shift search range limits $SR_{\min}$ and $SR_{\max}$ can all be varied in calculating the flow velocity. The only parameter which cannot be varied is the length of the correlation window, which is hard-wired at 40 in the RNS correlator. The value of the correlation parameters directly affects the speed and the accuracy of the flow velocity estimation. The more echo signals which are chosen for the analysis, for example (large E), the more accurate the analysis will be at the expense of a longer computation time.

Adjustable parameters The number of processed echoes E and the processed echo length EL are variable and can be different from the acquired values. EL corresponds to the ranges in the tissue in which the flow velocity is estimated across. A small vessel may occupy only a fraction of the acquired echo signal, hence processing of the entire echo would not be time-efficient.

The range increment R_i specifies the locations within the echo signal that 40-point correlations are processed. This can be set to increments of 40-, 20-, or 10-points (corresponding to 0.60, 0.30, and 0.15 mm axial spacings in tissue). Since a 40-point window corresponds to a 0.60 mm axial range in tissue; there is no overlap between the correlation windows at a 0.60-mm range increment. For a 0.30-mm range increment, there is a 50% overlap, and for a range increment of 0.15 mm, there is a 75% overlap. For a small vessel, R_i and EL can both be decreased by a factor of four, which would increase the measurement density but keep the overall speed the same. Note that decreasing R_i increases the measurement density (measurements per unit distance) though not strictly the axial resolution, which is the transmitted pulse length convolved with the correlation window length.

$\Delta_{\max}$ can be varied from 1 to 10, and $\Delta_{\max}$ and E determine the total number of echo pairs EP and individual velocity estimates used in averaging. For $\Delta_{\max} = 1$, there is no weighted averaging. With $\Delta_{\max} = 1$ and 101 echoes, for example, there will be a total number of echo pairs $EP = 100$ and 100 corresponding individual flow velocity estimates which are directly averaged. For $\Delta_{\max} = 10$ and $E = 110, EP = 1000$ and 1000 velocity estimates are weighted averaged according to (7). The performance of the

UTDC flowmeter, in terms of speed, accuracy, and precision, as a function of $\Delta_{\max}$ and E, is evaluated in Part II of this work [24].

The shift search range limits $SR_{\min}$ and $SR_{\max}$ are adjustable and define the range of shifts performed about the preshift S_p. A large range will in give a higher probability that a valid maximum will be found, again at the expense of processing time. A single shift equals 20 ns, which corresponds to a flow velocity of 1.5 cm at the 1-kHz PRF of the MK500. Thus if $SR_{\min} = -5$ and $SR_{\max} = +5$, the correlation coefficient will be calculated at shifts of $-5 \leq s \leq 5$ around S_p, and the estimate for τ will be valid as long as the axial velocity does not change by more than ± 7.5 cm/s from the previous measurement. $SR_{\min}$ and $SR_{\max}$, along with the PRF of the imager, define the maximum measurable axial flow velocity of the flowmeter. Since $\Delta = 1$ is used as the very first estimate (there is no preshift for $\Delta = 1$), the magnitude of the axial flow velocity cannot be greater than 7.5 cm/s for $SR_{\min} = -5$ and $SR_{\max} = 5$.

IV. Conclusion

A prototype UTDC blood flowmeter with a high-speed RNS correlator has been developed. The RNS correlator, along with a high amount of flexibility in choosing optimal values for the correlation parameters, allows one-dimensional blood flow velocity estimation to be made. Currently, only calculation of the correlation coefficients is performed in hardware, and the correlation search and parabolic curve fitting routines are still performed in software. Plans for future versions of the real-time UTDC blood flowmeter include hardware implementation of the entire correlation-search algorithm, as well as development of custom- designed VLSI RNS correlator chips. This will allow a flowmeter with parallel correlation channels to be constructed which will have the capability of producing two-dimensional flow velocity profiles in real time.

Appendix

Residue Number System Example

As an example of RNS correlation, suppose that the following simple two-sample correlation is to be performed:

$$(109) \times (47) + (-83) \times (12) = 4127 \tag{12}$$

The moduli and parameters are

$p_1 = 59 \quad m_1 = 245,952 \quad m_1^{-1} = 31$
$p_2 = 61 \quad m_2 = 237,888 \quad m_2^{-1} = 5$
$p_3 = 63 \quad m_3 = 230,336 \quad m_3^{-1} = 8$
$p_4 = 64 \quad m_4 = 226,737 \quad m_4^{-1} = 17$
$M = 14,511,168$

The residues for all 6-bit numbers are precalculated using (9) and stored in ROM's, as shown in Table I (shown only for values used in (12)). The natural numbers in terms of their moduli are

$$\begin{aligned} 109 &= \{50_{59}, 48_{61}, 46_{63}, 45_{64}\} \\ 47 &= \{47_{59}, 47_{61}, 47_{63}, 47_{64}\} \\ -83 &= \{35_{59}, 48_{61}, 43_{63}, 45_{64}\} \\ 12 &= \{12_{59}, 12_{61}, 12_{63}, 12_{64}\} \end{aligned}$$

TABLE I
6-Bit ROM Lookup Table

Value	mod 59 ROM	mod 61 ROM	mod 63 ROM	mod 64 ROM
12	12	12	12	12
47	47	47	47	47
109	50	48	46	45
-83 (173)	35	39	43	45

where each residue number within brackets is a 6-bit value. The correlation in the RNS domain becomes

$$\begin{aligned} y_{59} &= (50 \star 47 + 35 \star 12)_{59} \\ y_{61} &= (48 \star 47 + 39 \star 12)_{61} \\ y_{63} &= (46 \star 47 + 43 \star 12)_{63} \\ y_{64} &= (45 \star 47 + 45 \star 12))_{64} \end{aligned} \tag{13}$$

All of the multiplies in (13) are done using lookup tables stored in ROM. The two 6-bit numbers to be multiplied form an effective 12-bit address of a 4096×6 bit ROM. The value stored at the 12-bit address is the result of the multiplication of the individual two 6-bit residues. After the lookup-table multiplications, (13) becomes

$$\begin{aligned} y_{59} &= (49 + 7)_{59} = 56_{59} \\ y_{61} &= (60 + 41)_{61} = 40_{61} \\ y_{63} &= (20 + 12)_{63} = 32_{63} \\ y_{64} &= (3 + 28)_{64} = 31_{64} \end{aligned} \tag{14}$$

where y_{nn} are the residues of the result of the correlation. The natural result Y can then be computed using from (10):

$$\begin{aligned} Y &= |245,952 \star (31 \star 56)_{59} + 237,888 \star (5 \star 40)_{61} \\ &\quad + 230,336 \star (8 \star 32)_{63} \\ &\quad + 226,737 \star (17 \star 31)_{64}|_{\text{mod } 14,511,168} \\ &= |6,148,800 + 4,044,096 \\ &\quad + 921,344 + 3,401,055|_{\text{mod } 14,511,168} \\ &= |14,515,295|_{\text{mod } 14,511,168} \\ &= 4127\surd. \end{aligned}$$

References

[1] P. N. T. Wells, *Biomedical Ultrasonics*. New York: Academic Press, 1977.

[2] J. G. Webster, *Medical Instrumentation: Application and Design*. Boston: Houghton Mifflin, 1980.

[3] R. W. Gill, "Measurement of blood flow by ultrasound: Accuracy and sources of error," *Ultrasound Med. Biol.*, vol. 11., pp. 625–641, 1985.

[4] P. M. Embree and W.D. O'Brien, Jr., "Pulsed Doppler accuracy assessment due to frequency dependent attenuation and Rayleigh scattering error sources," *IEEE Trans. Biomed. Eng.*, vol. 37, pp. 322–326, Mar. 1990.

[5] I. A. Hein and W. D. O'Brien, Jr., "Current time-domain methods for assessing tissue motion by analysis from reflected ultrasound echoes (A Review)," *IEEE Trans. Ultrason. Ferro. Freq. Contr.*, vol. 40, pp. 1–19, Mar. 1993.

[6] R. J. Dickinson and C. R. Hill, "Measurement of soft tissue motion using correlation between A-scans," *Ultrasound Med. Biol.*, vol. 8, no. 3, pp. 263–271, 1982.

[7] M. Tristam, D. C. Barbosa, D.O. Cosgrove, J.C. Bamber, and C. R. Hill, "Application of Fourier analysis to clinical study of patterns of tissue movement," *Ultrasound Med. Biol.*, vol. 14, no. 8, pp. 695–707, 1988.

[8] J. Ophir, I. Cespedes, H. Ponnekanti, Y. Yazdi, and X. Li, "Elastography: A quantitative method for imaging the elasticity of biological tissues," *Ultrasonic Imaging* 13, pp. 111–134, 1991.

[9] R. S. Adler, J. M. Rubin, P. H. Bland, and P. L. Carson, "Quantitative tissue motion analysis of digitized M-mode images: Gestational differences in fetal lung," *Ultrasound Med. Biol.*, vol 16, no. 6, pp. 561–569, 1990.
[10] P. G. M. de Jong, T. Arts, A. P. G. Hoeks, and R. S. Reneman, "Determination of tissue motion velocity by correlation interpolation of pulsed ultrasonic signals," *Ultrasonic Imaging* 12, pp. 84–98, 1990.
[11] P. G. M. de Jong, T. Arts, A. P. G. Hoeks, and R. S. Reneman, "Experimental evaluation of the correlation interpolation technique to measure regional tissue velocity," *Ultrasonic Imaging* 8, pp. 145–161, 1991.
[12] D. Dotti, E. Gatti, V. Svelto, A. Ugge, and P. Vidali, "Blood flow measurement by ultrasound correlation techniques," *Energia Nucleare*, vol. 23, no. 11, pp. 571–575, Nov. 1976.
[13] S. G. Foster, P. M. Embree, and W. D. O'Brien Jr., "Flow velocity profile via time domain correlation: error analysis and computer simulation," *IEEE Trans. Ultrason. Ferro. Freq. Contr.*, vol. 37, pp. 164–175, May 1990.
[14] P. M. Embree, "Volumetric blood flow via time-domain correlation: Experimental verification," *IEEE Trans. Ultrason. Ferro. Freq. Contr.*, vol. 37, pp. 176–189, May 1990.
[15] I. A. Hein and W. D. O'Brien Jr., "Volumetric measurement of pulsatile flow via ultrasound time-domain correlation," *J. Cardiovascular Technology*, vol. 8, no. 4, pp. 339–348, 1989.
[16] O. Bonnefous, "Statistical analysis and time domain correlation processes applied to velocity measurement," in *IEEE 1989 Ultrasonics Symp. Proc.*, Montreal, Canada, Oct. 1989, pp. 887–892.
[17] O. Bonnefous and P. Pesque, "Time domain formulation of pulse-Doppler ultrasound and blood velocity estimation by cross correlation," *Ultrasonic Imaging* 8, pp. 73–85, 1986.
[18] K. W. Ferrara and V. R. Algazi, "A new wideband spread target maximum likelihood estimator for blood velocity estimation—Part I: Evaluation of estimators with experimental data," *IEEE Trans. Ultras. Ferroelec. Freq. Contr.*, vol. 38, pp. 1–16, Jan. 1991.
[19] K. W. Ferrara and V. R. Algazi, "A new wideband spread target maximum likelihood estimator for blood velocity estimation—Part II: Evaluation of estimators with experimental data," *IEEE Trans. Ultrason. Ferroelec. Freq. Contr.*, vol. 38, pp. 17–26, Jan. 1991.
[20] G. E. Trahey, S. M. Hubbard, and O. T. von Ramm, "Angle independent ultrasonic blood flow detection by frame-to-frame correlation of B-mode images," *Ultrasonics*, vol. 26, pp. 271–276, Sept. 1988.
[21] L. N. Bohs and G. E. Trahey, "A novel method for angle independent ultrasonic imaging of blood flow and tissue motion," *IEEE Trans. Biomed. Eng.*, vol. 38. pp. 280–286, Mar. 1991.
[22] D. Kim, T. M. Kinter, and J. F. Greenleaf, "Correlation search method with third-order statistics for computing velocities from ultrasound images," in*IEEE 1989 Ultrasonics Symposium Proceedings*, Montreal, Canada, 1989, pp. 869–872.
[23] I. A. Hein, "Measurement of volumetric blood flow using ultrasound time domain correlation," Ph. D. dissertation, Dept. of Electrical and Computer Engineering, Univ. of Illinois at Urbana-Champaign, Urbana, IL, 1990.
[24] I. A. Hein and W. D. O'Brien, Jr., "A real-time ultrasound time-domain correlation blood flowmeter part II: performance and experimental verification," submitted to IEEE Trans. Ultrason. Ferro. Freq. Contr.
[25] B. A. J. Angelson, "A theoretical study of the scattering of ultrasound from blood," *IEEE Trans. Biomed. Eng.*, vol. BME- 27. No. 2, 61–67, 1980.
[26] J. T. Chen, "Design and implementation of a high-speed residue number system correlator for ultrasonic time-domain blood flow measurement," M. S. thesis, Dept. of Electrical and Computer Engineering, University of Illinois at Urbana-Champaign, Urbana, IL, 1990.
[27] J. T. Chen, W. K. Jenkins, I. A. Hein, and W. D. O'Brien, Jr., "Design and implementation of a high-speed residue number system correlator for ultrasonic time-domain blood flow measurement," in *Proc. 1990 Int. Symp. on Circuits and Systems*, New Orleans, LA, May 1990, pp. 2893–2896.
[28] M. A. Soderstrand, W. K. Jenkins, G. A. Jullien, and F. J. Taylor, eds., *Residue Number System Arithmetic, Modern Applications in Digital Signal Processing*. New York: IEEE Press, 1986.

Ilmar A. Hein (S'90–M'90) was born in Woodstock, IL on August 15, 1959. He received the B.S., M.S., and Ph.D. degrees in electrical engineering from the University of Illinois at Urbana-Champaign in 1981, 1983, and 1990, respectively.

From 1983 to 1985, he worked as a microwave engineer at Hughes Aircraft Company in El Segundo, CA. From 1990 to 1992 he worked as a postdoctoral research associate at the University of Illinois on measurement of blood flow and tissue motion by ultrasound time-domain correlation and other bioengineering projects. He is currently an ultrasound scientist at Bio-Imaging Research, Inc. in Lincolnshire, IL, and an adjunct professor at the University of Health Sciences/Chicago Medical College in North Chicago, IL.

Dr. Hein is a member of the Acoustic Society of America and the American Institute of Ultrasound in Medicine (AIUM). He was awarded the Terrence Matzuk Memorial Award by AIUM for innovative research in the development of ultrasonic instrumentation and technology in 1988.

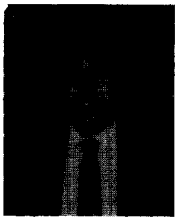

Jerome T. Chen (M'88) was born in February 1965 in Athens, OH. He received the B.S. degree in computer engineering in 1987 and the M.S. degree in electrical engineering in 1990, both from the University of Illinois at Urbana-Champaign, Urbana, IL.

He joined the Los Alamos National Laboratory as a Technical Staff Member in 1990, where his research interests include signal processing, communications, and sensors.

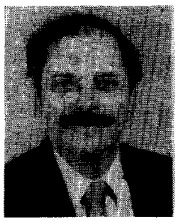

W. Kenneth Jenkins (F'85) received the B.S.E.E. degree from Lehigh University, Bethlehem, PA in 1969, and the M.S.E.E. and Ph.D. degrees from Purdue University, West Lafayette, IN in 1971 and 1974, respectively.

From 1974 to 1977, he was a Research Scientist Associate in the Communications Sciences Laboratory at the Lockheed Research Laboratory, Palo Alto, CA. In 1977, he joined the faculty at the University of Illinois at Urbana-Champaign, where he is currently a Professor in the Electrical and Computer Engineering Department and the Coordinated Sciences Laboratory. Since May 1987, he has been Director of the Coordinated Science Laboratory and Principal Investigator on the Joint Services Electronics Program (JSEP) at the University of Illinois. His current interests include digital filtering, signal processing algorithms, multidimensional array processing, computer imaging, one- and two-dimensional adapative digital filtering, and VLSI architectures for signal processing.

Dr. Jenkins is a past Associate Editor for IEEE TRANSACTIONS ON CIRCUITS AND SYSTEMS, and has served as the Secretary–Treasurer (1982–1983), President-Elect (1984), and President (1985) of the CAS Society. Also, he has served as General Chairman of the 32nd Midwest Symposium on Circuits and Systems (1988) and the Program Chairman of the 1990 IEEE International Symposium on Circuits and Systems. He is a member of Phi Eta Sigma, Eta Kappa Nu, and Tau Beta Pi. He was the recipient of the 1977 Lockheed Publication Award, and in 1978 was awarded the first Myril B. Reed Best Paper Award at the Midwest Symposium on Circuits and Systems. In 1980 he co-authored a paper on computer-aided analysis that received the fourth Myril B. Reed Best Paper Award. He received the 1985 ICCD Award at the International Conference on Circuits and Computers for the best technical presentation in Algorithms and Architectures. Also in 1985, he was elected Fellow of the IEEE for his professional contributions in digital signal processing and engineering education. In 1990, he was awarded the Distinquished Service Award of the IEEE Circuits and Systems Society for important and sustained professional contributions to the Society over many years.

William D. O'Brien, Jr. (S'64–M'71–SM'79–F'89), for a photograph and a biography, please see page 102 of the March 1993 issue of this TRANSACTIONS.